Bitlis Eren Üniversitesi Fen Bilimleri Dergisi
BİTLİS EREN UNIVERSITY JOURNAL OF SCIENCE
ISSN: 2147-3129/e-ISSN: 2147-3188
VOLUME: 13 NO: 4 PAGE: 969-978 YEAR: 2024
DOI: 10.17798/bitlisfen.1485060

NiO Nanoparticles Via Calcination of Dithiocarbamate Precursors: Characterization and Photocatalytic Activity

Ayşegül ŞENOCAK[1*], Hüseyin AKBAŞ[1], Beyza İŞGÖR[1]

[1] *Tokat Gaziosmanpaşa University, College of Art and Science, Department of Chemistry, Tokat, Türkiye*
ORCID: (0000-0001-9210-4621) (ORCID: 0000-0002-3013-9033) (ORCID: 0009-0000-9530-8750)

Keywords: Dithiocarbamates, NiO nanoparticles, Calcination, Photocatalytic activity, Methylene blue

Abstract
By this work, the preparation of NiO nanoparticles (NPs) from a dithiocarbamate complex through calcination, both a cost-effective and practical way for NPs synthesis, was presented. This preparation process involves the decomposition of the precursor to yield highly pure and crystalline NPs. The dithiocarbamate complex was synthesized in a sequential reaction starting from p-anisaldehyde and 3-aminopropanol. Particle size of the NPs, whose formation was confirmed by FT-IR spectroscopy and UV-Vis spectroscopy, were calculated as 10.97 nm using Debye-Scherer equation from X-ray Diffraction Spectroscopy (XRD). In addition, Scanning Electron Microscopy (SEM) revealed generally aggregated and spherical particles, which are stable in colloidal environment according to -15.1 zeta potential value. Besides, the NPs were employed as a photocatalyst for the decomposition of Methylene Blue (MB), one of the most frequently used synthetic dyes in industry and, at the same time, one of the primary water pollutants, resulting in 38% degradation rate.

1. Introduction

Dithiocarbamates, represented by the general formula S_2CNR_2, are a remarkable group of compounds, distinguished by their unique sulfur-sulfur bonds and a variety of intriguing properties. From their origins in the late 19th century to their contemporary members in diverse applications, dithiocarbamates have left an indelible mark on modern chemistry. Dithiocarbamate compounds possess an exceptional ability to easily capture a broad range of metal ions, allowing for the construction of complex architectures, which have brought in great importance to them in coordination chemistry. Synthesis of the dithiocarbamate complexes typically involves the preparation of the dithiocarbamate ligand through the reaction of amine compounds with CS_2 in a basic medium, followed by its coordination with a metal ion [1], [2], [3]. This process allows for convenient regulation of the electrical and structural characteristics of the final dithiocarbamate compound by manipulating the pioneer amine.

The resonance structures of dithiocarbamates allow them to readily coordinate with a wide range of metal ions (Figure 1). The thioureide form functions as a weak-field ligand, providing stability to high-valent metals. On the other hand, the dithiocarbamate form tends to capture low-valent metals as a strong-field ligand. Among the various coordination modes available to dithiocarbamates, the most common is the bidentate chelate, which enhances the stability of the resulting structure [4].

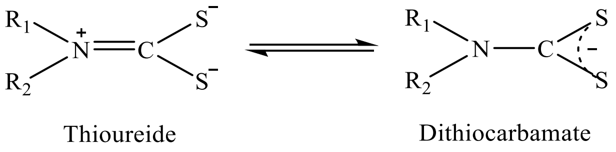

Figure 1. The resonance forms of dithiocarbamates.

---

[*] Corresponding author: aysegul.senocak@gop.edu.tr

Received: 16.05.2024, Accepted: 17.12.2024

Due to their strong affinity for metals, numerous dithiocarbamate complexes, demonstrating a broad range of applications including high-pressure lubricants and accelerators in vulcanization [5], anion sensors [6], sensitizers in solar schemes [7], pesticides and fungicides [8], [9], as well as anticancer, antibacterial, and antioxidant agents [10], [11], [12], have been synthesized. Nickel dithiocarbamate complexes, in particular, have been extensively examined for their biological activities, including anticancer, antimicrobial, or antioxidant [13], [14], [15], [16], [17]. Furthermore, numerous studies have focused on the utilization of dithiocarbamate complexes as single-source precursors for nickel NPs [18], [19], [20], [21], [22], [23]. Various methods were employed for nickel NPs production; for instance, in some of these studies, NiO NPs were generated through high-temperature calcination, while in the others, the solvothermal method was employed by adding ethylenediamine for nickel sulfide NPs synthesis [18].

NPs composed of NiO exhibit diverse applications across multiple disciplines, including energy storage [24], rechargeable batteries [25], catalysis [26], bio-active materials [27], and sensors [28]. In recent years, the catalytic activities of NiO NPs have gained great importance, particularly in environmental applications, due to the escalating pollution caused by rapid industrialization and uncontrolled population growth. One of the catalytic applications of NiO NPs pertains to degrading synthetic dyes present in water contaminated by industrial effluents. Numerous methods which can be classified as biological, chemical and physical have been used for remediation of contaminated waters with dyes. Among these methods, photocatalysis has garnered significant attention as it is the most effective and environmentally friendly approach to date [29]. Research in this area revealed that NiO NPs have exhibited successful results as photocatalysts in the breaking down industrial dyes such as MB, Rhodamine B, and Brown HT [30], [31], [32]. The degradation process occurs through the generation of O_2 and OH radicals within the positively charged cavities on the surface of NPs by means of electron excitation and the subsequent interaction of these radicals with synthetic dyes, leading to the decomposition of these dyes [33].

In this study, it was aimed to transform one example of the widely studied dithiocarbamate complexes into nickel NPs, which are utilized in addressing the nowadays pressing issue of environmental pollution. For this aim, a nickel dithiocarbamate complex was prepared through a chain reaction starting with 4-methoxybenzaldehyde and 3-aminopropanol. The resulting complex was then thermally decomposed to produce NiO NPs, which were characterized by using FT-IR, UV-Vis, SEM-EDS, XRD, and Zeta Potential methods. Besides, the photocatalytic capacity of the NPs over the decomposition of MB was evaluated.

2. Material and Method

4-methoxybenzaldehyde (98%), 3-aminopropanol (99%), sodium borohydride (98%), potasium hydroxide (99%), carbon disulfide (99%), nickel(II) sulfate hexahydrate (98%), methylene blue (82%), dicholoromethan, and ethanol were purchased and used without any additional purification procedure. The FT-IR spectra were measured between 400-4000 cm^{-1} range using a Jasco FTIR 4700 spectrometer. By employing a Perkin-Elmer Lambda-35 UV-Vis spectrophotometer, which operates in the range of 200–800 nm, the UV-Vis spectra of the nickel complex and NPs in ethanol (10^{-3} M) were recorded. The XRD pattern was recorded using a PANalytical X-Pert3 Powder X-ray diffractometer with Cu-Kα radiation. The morphological characters of the NPs were investigated using a TESCAN™ MIRA3 XMU SEM. In order to determine the zeta potential of the NPs dispersed in ultra-pure water, the Malvern/Zetasizer Nano ZSP utilized the diffusion light scattering approach.

2.1. Preparation of the Nickel Dithiocarbamate Complex

4-methoxybenzaldehyde and 3-aminopropanol in equimolar amounts were refluxed in methanol for 4 days. Once the transformation into the Schiff base was complete, excess sodium borohydride was added to the reaction mixture in small portions. After the reduction was finished, the methanol was evaporated from the crude product. The resulting oily product was washed twice with a CH_2Cl_2/water mixture and dried over Na_2SO_4, heated in a muffle furnace at 250 ºC.

The final reduced amine in light yellow, oily form was dissolved in ethanol and cooled to 0 ºC. To this solution, KOH and CS_2 in ethanol were added dropwise, respectively. After stirring for a day at room temperature, the appearance of the yellow solution indicated the dithiocarbamate formation. Subsequently, an aqueous solution of $NiSO_4.6H_2O$ (0.5 equivalent) was added to form the complex structure. A green precipitate formed immediately was filtered after stirring for one day, and the residue on the filter paper was allowed to dry and was then isolated.

2.2. Preparation of the NiO NPs

The resulting complex was placed in porcelain crucibles and calcined in a muffle furnace at 500 ºC for 4 hours. Distilled water was added to the resulting substance and mixed at 80 ºC for 20 minutes. Then, the mixture was transferred to centrifuge tubes and centrifuged for 3 minutes. The decanted NPs were centrifuged further 3 minutes after being washed with ethanol. The obtained NiO NPs were left to dry at room temperature and isolated.

2.3. Photocatalytic Performance

A batch process was employed to study the photocatalytic activity and decomposition kinetics of the NiO NPs in the degradation of MB. With this aim, NiO NPs (20 mg), predried at 100 ºC for 2 hours, were added to 10 ppm MB solution (50 mL), and this mixture was stirred magnetically in the dark for an hour to reach thermodynamic equilibrium. Then, the reaction vessel was opened to light and allowed to mix under a daylight lamp (10 watt) positioned 30 cm above the reaction surface. The UV spectrum of the resulting solution was measured by withdrawing 3 mix under a daylight lamp (10 watt) positioned 30 cm above the reaction surface. The UV spectrum of the resulting solution was measured by withdrawing 3 mL samples every hour. The results were interpreted by calculating the amount of MB remaining in the solution by using Eq. 1 where A_0 an A_t represent the initial absorbtion and absorbtion at time t, respectively.

$$\boldsymbol{Dye\ Removal} = \left({}^{(\boldsymbol{A_0} - \boldsymbol{A_t})}\!/_{\boldsymbol{A_0}} \right) * \mathbf{100} \qquad (1)$$

3. Results and Discussion

In this research, a nickel dithiocarbamate complex was obtained by sequential reactions starting with 4-methoxybenzaldehyde and 3-aminopropanol, and the final complex was then subjected to calcination to produce NiO NPs (Scheme 1). A color transformation from green to gray was observed as a consequence of the calcination process (Figure 2). The structure of the resulting NiO NPs was illuminated by a number of spectroscopic techniques, involving FT-IR, UV-Vis, XRD, SEM-EDX, and zeta potential.

Figure 2. Powder forms of the dithiocarbamate complex (green) and the NiO NPs (gray).

As the first step of characterization, the FT-IR and UV-Vis spectra of the dithiocarbamate complex and the NiO NPs were measured and compared to assess the appearance and purity of the NPs. The FT-IR spectra of the dithiocarbamate complex and the final NPs were depicted in Figure 3. One of the key features in the spectrum was the coordinated O-H stretching observed between 3671-3007 cm^{-1}. The splitting of the C-S band (981 and 961 cm^{-1}) gave rise to the hypothesis that the dithiocarbamate group coordinated with the Ni(II) ions in a monodentate manner [34]. Besides, the band at 1501 cm^{-1} emphasized the partial double bond character of the C-N bond, while Ni-S bond formation was confirmed by the peak at 508 cm^{-1} [7]. Considering all these provided spectroscopic evidence, the structural formula for the nickel dithiocarbamate complex was proposed as shown in Scheme 1. The disappearance of all characteristic bands of the pioneer complex in the FT-IR spectrum emphasized the complete conversion of the nickel complex into NPs as a result of calcination. Furthermore, the band at 406 cm^{-1} provided evidence of the existence of NiO NPs in accordance with previous studies [35], [36], [37].

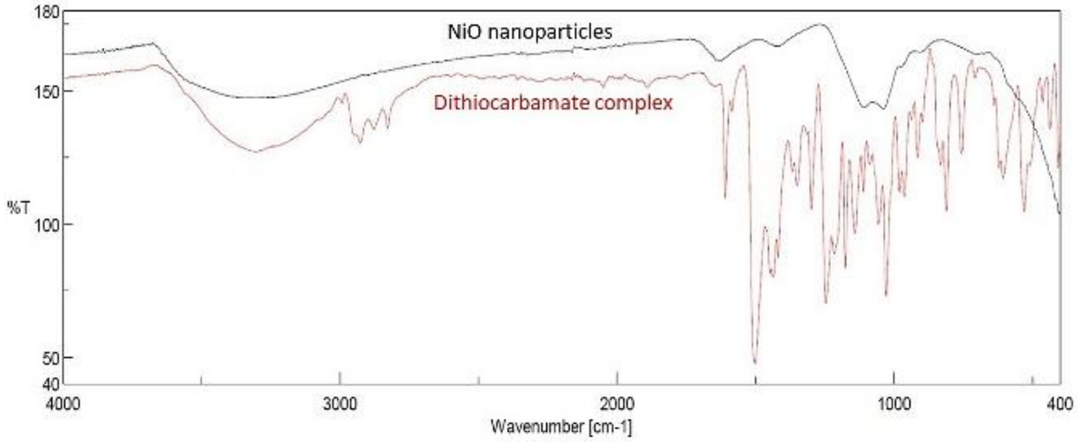

Figure 3. FT-IR spectra of the dithiocarbamate complex and NPs.

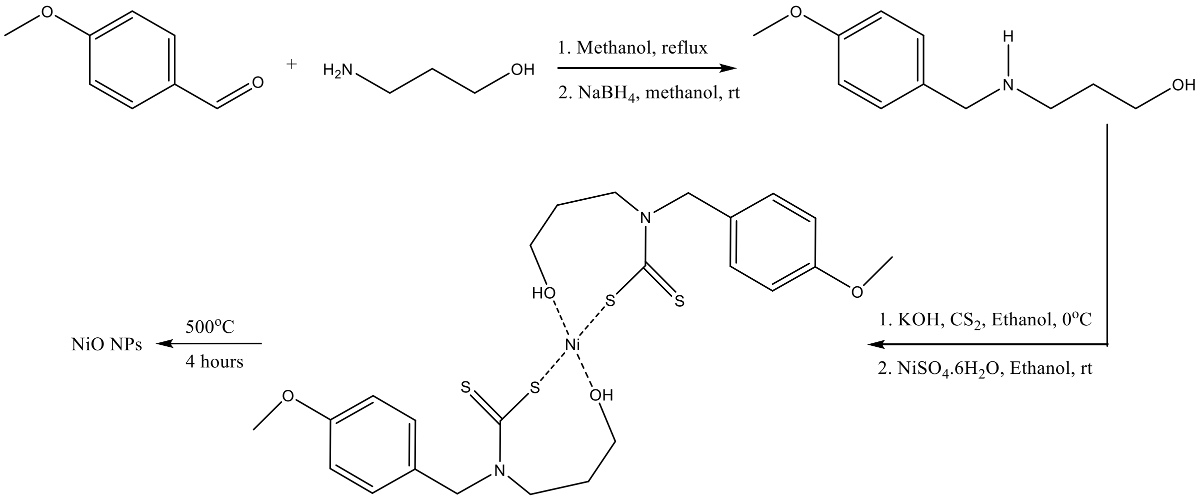

Scheme 1. The reaction scheme and the proposed complex structure for the production of NiO NPs.

The UV-Vis spectra of the nickel complex and the NiO NPs dispersed in ethanol by an ultrasonic bath were depicted in Figure 4.

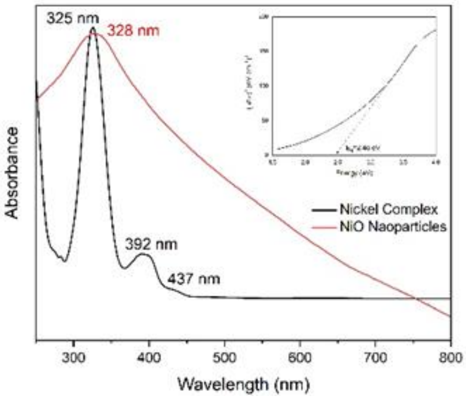

Figure 4. UV-Vis spectra of the complex and the NPs (with $(Ah\upsilon)^2$–$h\upsilon$ plot (inset)).

Two absorbtion maxima at 325 and 392 nm were assigned to metal-ligand charge transfer for square planar complexes. Besides, a d-d transition in the metal center was observed as a shoulder at 437 nm [38]. The UV maxima at 328 nm pointed out the presence of the NiO NPs in line with their counterparts in the previous studies [39], [40], [41]. Furthermore, to calculate the optical band gap of the NPs, a Tauc plot was included in the UV-Vis spectrum. The band gap energy was determined as 2.46 eV from the graph drawn by employing the $(Ah\upsilon)^2 = B(h\upsilon\text{–}Eg)$ equation, where A is the absorption coefficient and B is a constant. The band gap energy, an indicator for the ease of electron jump from the valence band to the conduction band, is compatible with the literature [42], [43].

The XRD spectrum of the NPs exhibited diffraction peaks at 37.43 [1 1 1], 43.35 [2 0 0], 63.01 [2 2 0], 75.61 [3 1 1], 79.59 [2 2 2] (Figure 5). XRD analysis confirmed that the nanoparticle crystallized in a Bunsenite structure, identified with COD 98-002-8834, which corresponds to a cubic structure with space group Fm-3m. Besides, the density of the NiO NPs was calculated as 6.84

g/cm^3 based on the collected XRD data. Any impurities originated from the starting compound were not exhibited in the XRD pattern. Besides, the sharpness and intensities of the diffraction peaks pointed out the crystallinity of the NPs. The average radius of the obtained NPs was calculated as 10.97 nm by the Scherer equation, where λ is the wavelength of Cu-Kα, β is full width at the half max of the main peak, and θ is Bragg's angle (Equation 2).

$$\boldsymbol{D = (0.9 * \lambda)/(\beta * cos\theta)} \tag{2}$$

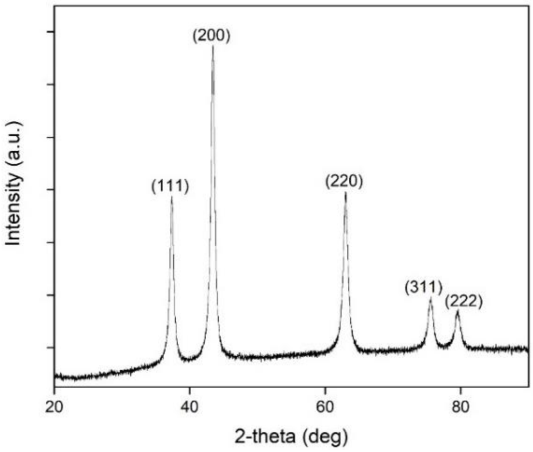

Figure 5. X-ray diffraction pattern for the synthesized NPs.

The images of the NiO NPs captured by the scanning electron microscope were exhibited in Figure 6. The particles were observed to have a generally spherical shape with an average size of 61.14 nm. It was also observed that NiO NPs aggregated as expected since no anti-collapse agent was used to minimize the interaction between the particles.

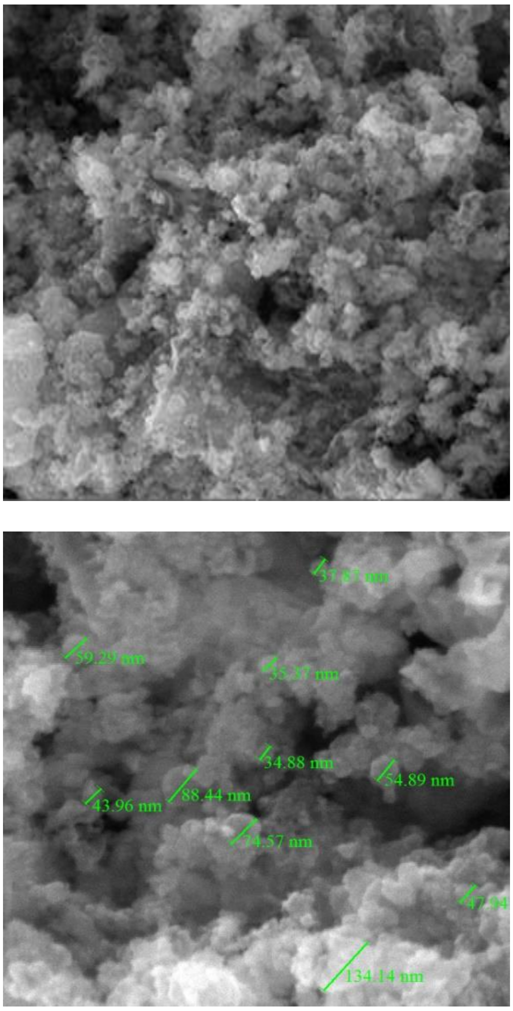

Figure 6. SEM micrograms of the NiO NPs.

EDS analysis revealed that the synthesized NPs were composed of 68.93% Ni and 25.21% O, which closely align with the theoretical ratios (78% Ni, 21% O) for the NiO general formula (Figure 7). The other elements (C, S, and K) observed in negligible amounts in the analysis results were attributed to instrumental impurities.

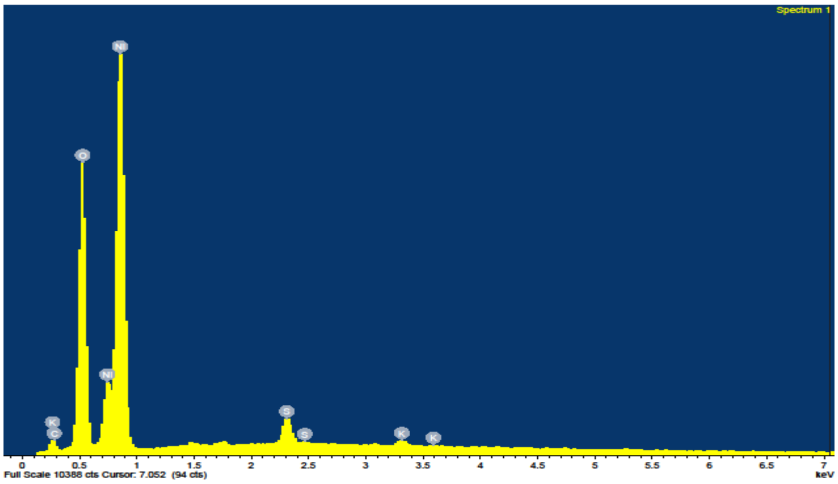

Element	Weight%	Atomic%
C K	3.97	10.53
O K	25.21	50.23
S K	1.50	1.49
K K	0.39	0.32
Ni K	68.93	37.43
Totals	100.00	

Figure 7. EDS spectrum of the NPs.

Zeta potential is a widely used criterion for interpreting the stability of NPs by providing information regarding the repulsion between similarly charged NPs in a colloidal environment. The more negative zeta potential value means greater stability of the NPs [44]. The -15.1 zeta potential value found in this study indicates that the prepared NiO NPs are stable in the colloidal environment (Figure 8).

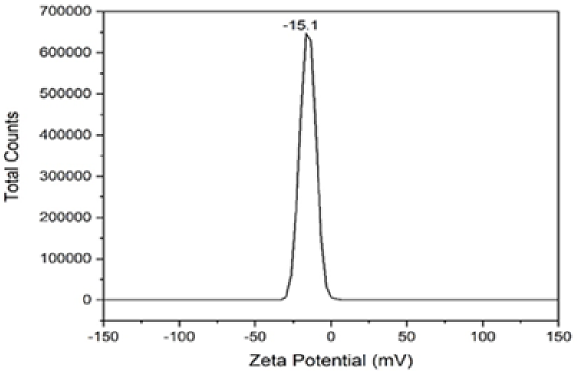

Figure 8. The zeta potential distribution of the NPs.

The photocatalytic activity of the characterized NiO NPs was evaluated for the decomposition of MB synthetic dye. The usage of NiO NPs in catalytic amounts in the presence of light from a daylight lamp ended up decomposition of 38% of MB over six hours (Figure 9). In addition, almost identical “before catalyst” and “0 min” spectra revealed that both light and the catalyst are essential for MB degradation. This moderate activity of the NPs emerged from the formation of positive holes based on electron motion between the energy bands of the NiO NPs by reason of exposure to sunlight and the transformation of methylene blue into small harmless molecules via the radicals forming in these cavities.

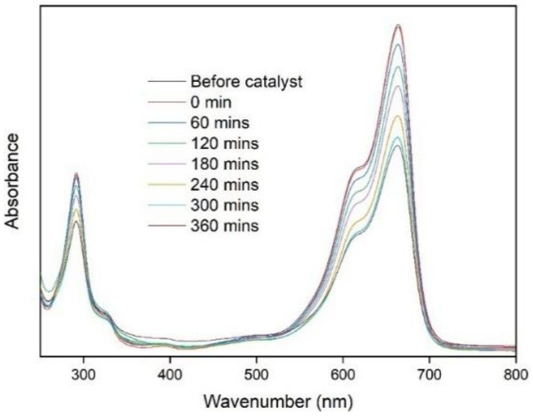

Figure 9. The NiO catalyzed photocatalytic degradation of MB over time.

By using Eq. 3, where C_t, C_0, and t represented the concentration at time t, the initial concentration, and time, the pseudo-first-order decomposition kinetics were examined for MB. The rate constant for the decomposition was calculated as 0.0014 min^{-1} (R^2= 0.982) which is lower than those in the previous study (Fig 10) [45].

$$\boldsymbol{ln} \, {}^{\boldsymbol{C_t}}\!/_{\boldsymbol{C_0}} = -\boldsymbol{k.t} \tag{3}$$

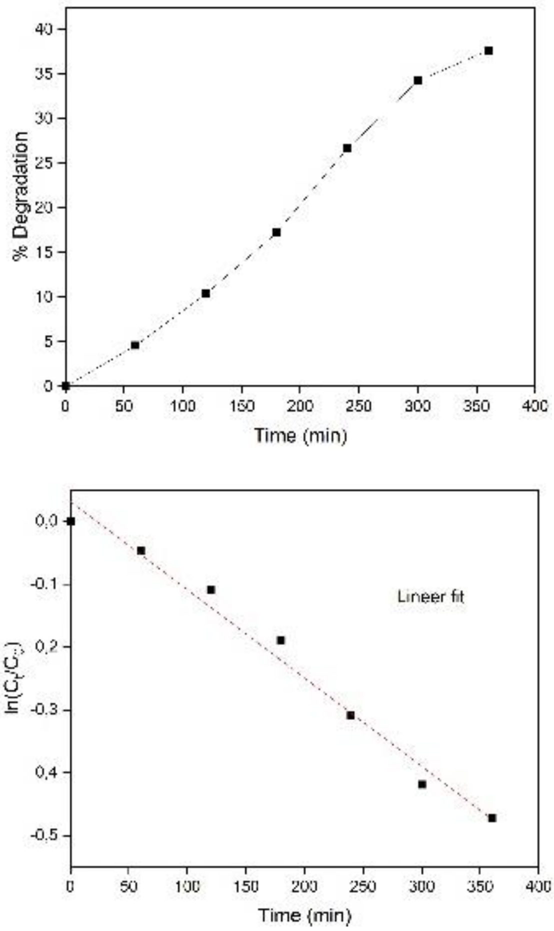

Figure 10. (a) The NiO catalyzed percentage degradation of MB **(b)** Pseudo-first-order kinetics for the MB decomposition.

4. Conclusion

In this study, NiO NPs were produced using the thermal decomposition (calcination) method from a nickel complex synthesized through a series of chemical reactions. The characterization of the synthesized NPs was carried out by FT-IR, UV-Vis, SEM, EDS, XRD, and Zeta Potential analyses. The values of 405 cm^{-1} and 328 nm observed in the FT-IR and UV-Vis spectra, respectively, are compatible with NiO NPs synthesized in the literature. Besides, XRD and EDS spectra further confirmed the formation of NiO NPs. By utilizing the XRD spectrum, the dimensions of the synthesized particles were calculated as 10.97 nm and, the sharpness of the XRD peaks was referred to the high crystallinity of the NPs. The SEM micrograph revealed non-uniform shaped and highly aggregated particles, which have an average size of 61.14 nm. The particle size from SEM micrograph was observed greater from those calculated by Debye-Scherer equation. The reason for this discrepancy may spring from the fact that XRD analysis determines the average size of the crystalline domains, whereas SEM spectroscopy measures the size of the individual particles. Besides, SEM spectroscopy can detect agglomerates, which can lead to an overestimation of the grain size. In contrast, the Scherer equation considers a perfect crystalline structure not agglomerates. The zeta potential value of -15.1 indicated that the synthesized NPs remained stable in the colloidal environment. Finally, the catalytic activity of the NiO NPs was evaluated for the degradation of MB under daylight lamp where the NPs exhibited moderate (38 %) photocatalytic activity.

Contributions of the authors

Ayşegül Şenocak contributed to the experimental studies, data interpretation, and the preparation of the manuscript.
Hüseyin Akbaş contributed to the experimental studies and the preparation of the manuscript.
Beyza İşgör contributed to the experimental studies.

Acknowledgment

The authors would like to thank to TUBİTAK (the Scientific and Technological Research Council of Türkiye) for supporting this study through the 2209-A Research Project Support Programme for Undergraduate Students (Project Number: 1919B012206215).

Conflict of Interest Statement

There is no conflict of interest between the authors.

Statement of Research and Publication Ethics

The study is complied with research and publication ethics.

References

[1] S. D. Oladipo, B. Omondi, and C. Mocktar, “Synthesis and structural studies of nickel(II)- and copper(II)-N,N′-diarylformamidine dithiocarbamate complexes as antimicrobial and antioxidant agents”, *Polyhedron*, vol. 170, pp. 712-722, 2019.

[2] G. Hogarth, “Metal-dithiocarbamate complexes: chemistry and biological activity”, *Mini-Rev. Med. Chem.*, vol. 12, no. 12, pp. 1202-1215, 2012.

[3] M. Shahid, T. Rüffer, H. Lang, S. A. Awan, and S. Ahmad, “Synthesis and crystal structure of a dinuclear zinc(II)-dithiocarbamate complex, bis{[(μ^2-pyrrolidinedithiocar-bamato-S,S’)(pyrrolidinedithio- carbamato-S,S’)zinc(II)]}”, *J. Coord. Chem.*, vol. 62, no. 3, pp. 440-445, 2009.

[4] J. C. Sarker, and G. Hogarth, “Dithiocarbamate Complexes as Single Source Precursors to Nanoscale Binary, Ternary and Quaternary Metal Sulfides”, *Chem. Rev.*, vol. 121, no. 10, pp. 6057-6123, 2021.

[5] T. A. Saiyed, J. O. Adeyemi, and D. C. Onwudi, “The structural chemistry of zinc(II) and nickel(II) dithiocarbamate complexes”, *Open Chem.*, vol. 19, pp. 974-986, 2021.

[6] P. D. Beer, A. G. Cheetham, M. G. B. Drew, O. D. Fox, E. J. Hayes, and T. D. Rolls, “Pyrrole-based metallo-macrocycles and cryptands”, *Dalton T.*, pp. 603-61, 2003.

[7] E. Sathiyaraj, G. Gurumoorthy, and S. Thirumaran, “Nickel(II) dithiocarbamate complexes containing the pyrrole moiety for sensing anions and synthesis of nickel sulfide and nickel oxide nanoparticles”, *New J. Chem.*, vol. 39, pp. 5336-5349, 2015.

[8] P. Ferreira, G. M. Lima, E. B. Paniago, J. A. Takahashi, and C. B. Pinheiro, “Synthesis, characterization and antifungal activity of new dithiocarbamate-based complexes of Ni(II), Pd(II) and Pt(II)”, *Inorg. Chim. Acta,* vol. 423(A), pp. 443-449, 2014.

[9] V. A. Fitsanakis, V. Amarnath, J. T. Moore, K. S. Montine, J. Zhang, and T. J. Montine, “Catalysis of catechol oxidation by metal-dithiocarbamate complexes in pesticides”, *Free Radical Bio. and Med.*, vol. 33, no. 12, pp. 1714-1723, 2002.

[10] D. C. Onwudiwe, and A. C. Ekennia, “Synthesis, characterization, thermal, antimicrobial and antioxidant studies of some transition metal dithiocarbamates”, *Res. Chem. Intermediat.*, vol. 43, pp.1465-1485, 2017.

[11] S. M. Mambaa, A. K. Mishraa, B. B. Mambaa, P. B. Njobehb, M. F. Duttonb, and E. Fosso-Kankeu, “Spectral, thermal and in vitro antimicrobial studies of cyclohexylamine-N-dithiocarbamate transition metal complexes”, *Spectrochim. Acta A*, vol. 77, pp. 579-587, 2010.

[12] I. Ali, W. A. Wani, K. Saleem, and M. -F. Hseih, “Design and synthesis of thalidomide based dithiocarbamate Cu(II), Ni(II) and Ru(III) complexes as anticancer agents”, *Polyhedron,* vol. 56, pp. 134-143, 2013.

[13] S. Balakrishnan, S. Duraisamy, M. Kasi, S. Kandasamy, R. Sarkar, and A. Kumarasamy, “Syntheses, physicochemical characterization, antibacterial studies on potassium morpholine dithiocarbamate nickel (II), copper (II) metal complexes and their ligands”, *Heliyon,* vol. 5, no. 5, pp. e01687, 2019.

[14] A. C. Ekennia, D. C. Onwudiwe, and A. A. Osowole, “Spectral, thermal stability and antibacterial studies of copper, nickel and cobalt complexes of N-methyl-N-phenyl dithiocarbamate”, *J. Sulfur Chem.*, vol. 36, no. 1, pp. 96-104, 2015.

[15] A. Pastrana-Dávila, A. Amaya-Flórez, C. Aranaga, J. Ellena, M. Macías, E. Flórez-López, and R. F. D'Vries, “Synthesis, characterization, and antibacterial activity of dibenzildithiocarbamate derivates and Ni(II)–Cu(II) coordination compounds”, *J. Molec. Struct.*, vol. 1245, pp. 131109, 2021.

[16] A. Singh, L. B. Prasad, K. Shiv, R. Kumar, and S. Garai, “Synthesis, characterization, and in vitro antibacterial and cytotoxic study of Co(II), Ni(II), Cu(II), and Zn(II) complexes of N-(4-methoxybenzyl) N-(phenylethyl) dithiocarbamate ligand”, *J. Molec. Struct.*, vol. 1288, pp. 135835, 2023.

[17] M. M. Hrubaru, E. Bartha, A. C. Ekennia, S. N. Okafor, C. D. Badiceanu, D. A. Udu, D. C. Onwudiwe, S. Shova, and C. Draghici, “Ni(II), Pd(II) and Pt(II) complexes of N,N-bis(3,3-dimethyl-allyl)-dithiocarbamate: Synthesis, spectroscopic characterization, antimicrobial and molecular docking studies”, *J. Molec. Struct.*, vol. 1250, no. 1, pp. 131649, 2022.

[18] A. Nqombolo, and P. A. Ajibade, “Synthesis and Spectral Studies of Ni(II) Dithiocarbamate Complexes and Their Use as Precursors for Nickel Sulphides Nanocrystals”, *J. Chem.-NY,* vol. 2016, pp. 1293790, 2016.

[19] D. C. Onwudiwe, N. H. Seheri, L. Hlungwani, H. Ferjani, and R. Rikhotso-Mbungela, “NiO nanoparticles by thermal decomposition of complex and evaluation of the structural, morphological, and optical properties”, *J. Mol. Struct.*, vol 1317, pp. 139084, 2024.

[20] V. K. Maurya, L. B. Prasad, A. Singh, K. Shiv, and A. Prasad, “Synthesis, spectroscopic characterization, biological activity, and conducting properties of functionalized Ni(II) dithiocarbamate complexes with solvent extraction studies of the ligands” *J. Sulphur Chem.*, vol 44 no.3, pp 336–353, 2022.

[21] E. Sathiyaraj, S. Thirumaran, S. Ciattini, and S. Selvanayagam, "Synthesis and characterization of Ni(II) complexes with functionalized dithiocarbamates: New single source precursors for nickel sulfide and nickel-iron sulfide nanoparticles", *Inorg. Chim. Acta*, vol. 498, pp. 119162, 2019.

[22] F. F. Bobinihi, O. E. Fayemi, and D. C. Onwudiwe, "Synthesis, characterization, and cyclic voltammetry of nickel sulphide and nickel oxide nanoparticles obtained from Ni(II) dithiocarbamate", *Mater. Sci. Semicond. Process*., vol. 121, pp. 105315, 2021.

[23] P. Lakshmanan, R. Arulmozhi, S. Thirumaran, and S. Ciattini, "Ni(II) dithiocarbamate: Synthesis, crystal structures, DFT studies and applications as precursors for nickel sulfide and nickel oxide nanoparticles", *Polyhedron*, vol. 218, pp. 115766, 2022.

[24] H. Wu, Y. Wang, C. Zheng, J. Zhu, G. Wu, and X. Li, "Multi-shelled NiO hollow spheres: Easy hydrothermal synthesis and lithium storage performances", *J. Alloy. Comp*., vol. 685, pp. 8-14, 2016.

[25] K. N. Patel, M. P. Deshpande, V. P. Gujarati, S. Pandya, V. Sathe, and S. H. Chaki, "Structural and optical analysis of Fe doped NiO nanoparticles synthesized by chemical precipitation route", *Mater. Res. Bull*., vol. 106, pp. 187-196, 2018.

[26] G. Grivani, M. Vakili, A. D. Khalaji, G. Bruno, H. A. Rudbari, M. Taghavi, and V. Tahmasebi, "Synthesis, characterization, crystal structure determination, computational study, and thermal decomposition into NiO nano-particles of a new $Ni^{II}L_2$ Schiff base complex (*L* = 2-{(E)-[2-chloroethyl)imino] methyl phenolate)", *J. Molec. Struct*., vol. 1072, pp. 77-83, 2014.

[27] K. Karthik, S. Dhanuskodi, C. Gobinath, S. Prabukumar, and S. Sivaramakrishnan, "Multifunctional properties of microwave assisted CdO–NiO–ZnO mixed metal oxide nanocomposite: enhanced photocatalytic and antibacterial activities", *J. Mater. Sci.-Mater. El.*, vol. 29, pp. 5459-5471, 2018.

[28] A. Salehirad, "Synthesis of high surface area NiO nanoparticles through thermal decomposition of mixed ligand Ni(II) Complex, [Ni(binol)(bpy)].CH_3OH", *Russ. J. Appl. Chem*., vol. 89, pp. 63-69, 2016.

[29] H. Kumari, Sonia, Suman, R. Ranga, S. Chahal, S. Devi, S. Sharma, S. Kumar, P. Kumar, S. Kumar, A. Kumar, and R. Parmar, "A Review on Photocatalysis Used For Wastewater Treatment: Dye Degradation", *Water Air Soil Pollut.*, vol. 234, no.6, pp. 349, 2023.

[30] M. Y. Nassar, H. M. Aly, E. A. Abdelrahman, and M. E. Moustafa, "Synthesis, characterization, and biological activity of some novel Schiff bases and their Co(II) and Ni(II) complexes: A new route for Co3O4 and NiO nanoparticles for photocatalytic degradation of methylene blue dye", *J. Mol. Struct.*, vol. 1143, pp. 462-471, 2017.

[31] Z. Sabouri, A. Akbari, H. A. Hosseini, M. Khatami, and M. Darroudi, "Egg white-mediated green synthesis of NiO nanoparticles and study of their cytotoxicity and photocatalytic activity", *Polyhedron*, vol. 178, pp. 114351, 2020.

[32] M. Darbandi, M. Eynollahi, N. Badri, M. F. Mohajer, and Z. A. Li, "NiO nanoparticles with superior sonophotocatalytic performance in organic pollutant degradation", *J. Alloy. Comp*., vol. 889, pp. 161706, 2021.

[33] Z. Sabouri, A. Akbari, H. A. Hosseini, A. Hashemzadeh, and M. Darroudi, "Bio-based synthesized NiO nanoparticles and evaluation of their cellular toxicity and wastewater treatment effects", *J. Molec. Struct.*, vol. 1191, pp. 101-109, 2019.

[34] E. Sathiyaraj, P. Valarmathi, S. Thirumaran, S. Ciattini, V. K. Gupta, and R. Kant, "Effect of N-Bound Organic Moiety in Dithiocarbamate (R2NCS−2) and trans Influence of Triphenylphosphine on NiS2PN Chromophore", *Phosphorus, Sulfur Relat. Elem*., vol. 190, no. 7, pp. 1127-1137, 2015.

[35] M. Abdur Rahman, R. Radhakrishnan, and R. Gopalakrishnan, “Structural, optical, magnetic and antibacterial properties of Nd doped NiO nanoparticles prepared by co-precipitation method”, *J. Alloy. Comp.*, vol. 742, pp. 421-429, 2018.

[36] M. A. J. Kouhbanani, Y. Sadeghipour, M. Sarani, E. Sefidgar, S. Ilkhani, A. M. Amani, and N. Beheshtkhoo, “The inhibitory role of synthesized Nickel oxide nanoparticles against Hep-G2, MCF-7, and HT-29 cell lines: the inhibitory role of NiO NPs against Hep-G2, MCF-7, and HT-29 cell lines”, *Green Chem. Lett. Rev.*, vol. 14, no. 3, pp. 444-454, 2021.

[37] E. Gobinath, M. Dhatchinamoorthy, P. Saran, D. Vishnu, R. Indumathy, and G. Kalaiarasi, “Synthesis and characterization of NiO nanoparticles using Sesbania grandiflora flower to evaluate cytotoxicity”, *Results Chem.*, vol. 6, pp. 101043, 2023.

[38] F. F. Bobinihi, D. C. Onwudiwe, and E. C. Hosten, “Synthesis and characterization of homoleptic group 10 dithiocarbamate complexes and heteroleptic Ni(II) complexes, and the use of the homoleptic Ni(II) for the preparation of nickel sulphide nanoparticles”, *J. Molec. Struct.*, vol. 1164, pp. 475-485, 2018.

[39] A. A. Barzinjy, S. M. Hamad, S. Aydın, M. H. Ahmed, and F. H. S. Hussain, “Green and eco-friendly synthesis of Nickel oxide nanoparticles and its photocatalytic activity for methyl orange degradation”, *J. Mater. Sci.-Mater. El.*, vol. 31, pp. 11303-11316, 2020.

[40] R. S. Kumar, S. J. Jeyakumar, M. Jothibas, I. K. Punithavathy, and J. P. Richard, “Influence of molar concentration on structural, optical and magnetic properties of NiO nanoparticles”, J. Mater. Sci.-Mater. El., vol. 28, pp. 15668-15675, 2017.

[41] M. El-Kemary, N. Nagy, and I. El-Mehasseb, “Nickel oxide nanoparticles: Synthesis and spectral studies of interactions with glucose”, *Mater. Sci. Semicond. Process.,* vol. 16, pp. 1747-1752, 2013.

[42] A. K. Ramasami, M. V. Reddy, and G. R. Balakrishna, “Combustion synthesis and characterization of NiO nanoparticles”, *Mater. Sci. Semicond. Process.*, vol. 40, pp. 194-202, 2015.

[43] F. Ascencio, A. Bobadilla, and R. Escudero, “Study of NiO nanoparticles, structural and magnetic characteristics”, *Appl. Phys. A*, vol. 125, pp. 279, 2019.

[44] A. B. García, A. Cuesta, M. A. Montes-Morán, A. Martínez-Alonso, and J. M. D. Tascón, “Zeta Potential as a Tool to Characterize Plasma Oxidation of Carbon Fibers”, *J. Colloid. Interf. Sci.*, vol. 192, pp. 363-367, 1997.

[45] K. Motene, L. Mahlaule-Glory, N. Ngoepe, M. Mathipa, and N. Hintsho-Mbita, “Photocatalytic degradation of dyes and removal of bacteria using biosynthesised flowerlike NiO nanoparticles”, *Int. J. Environ. Anal. Chem.*, vol. 103, no. 5, pp. 1107-1122, 2021.